Interaction Analysis in Islanded Power Systems with HVDC Interconnections

Carlos Collados-Rodríguez, Eduardo Prieto-Araujo,
Marc Cheah-Mane, Ricard Ferrer-San-José,
Oriol Gomis-Bellmunt
CITCEA-UPC, Spain
Email: carlos.collados@citcea.upc.edu

Silvia Sanz, Carmen Longás,
Antonio Cordón, Luis Coronado
Red Eléctrica de España, Spain

***Abstract*—Islanded power systems are often connected to larger mainland power systems using HVDC cables. The proliferation of new HVDC interconnectors in those islanded systems might lead to a reduction of the conventional synchronous generation-based power plants connected to the grid, with the associated decrease of rotating inertia and short-circuit current capacity in the resulting system, posing new challenges on the system stability and the behavior during system faults. In these situations, the power system dynamics heavily depend on the converter control algorithms, fact that requires new methodologies to study the system stability and the potential interactions between the different system elements, considering the power electronics. This paper analyses interactions in a multi-infeed HVDC islanded system with LCC and VSC-HVDC links. In particular, frequency stability is evaluated in a case study that represents an island with two HVDC links, two synchronous generators and an aggregated load. Also, frequency stability limits are determined when the synchronous generation of the island is reduced.**

I. Introduction

The number of power electronic devices connected to the grid is increasing due to the integration of renewable generation and High Voltage Direct Current (HVDC) transmission systems. An example of a grid with high penetration of converters is found in Northern Europe, where several countries and offshore wind power plants are connected through HVDC transmission systems. Areas with high penetration of power electronics present new challenges in relation to system stability and response during faults. In particular, instabilities might be caused by interactions between power converters and other components of the grid, *e.g.* transformers and transmission lines [1]–[5]. The converter control plays a key role to ensure a proper operation of the system and avoid undesirable interactions between components. Systems with multiples LCC-HVDC links have been studied in [6]–[8], where five main interactions are identified: transient overvoltage, commutation failure, harmonic interaction, power voltage stability and control interactions. Also, frequency stability may be considered in case of small systems with low inertia [8]. In order to limit the impact of these interactions, mitigation strategies were proposed based on converter design and control coordination [7].

A number of HVDC links has been used to connect islanded systems to the main AC grid. Interconnecting islands to mainland is a solution to reduce the high costs of local generation and improve the security of supply. In these cases, conventional power plants based on synchronous generators can be removed from the grid, reducing the inertia and short-circuit current capacity in the islanded system. Currently, most of the islanded systems interconnected through HVDC are based on Line-Commutated Converters (LCC): Gotland [9], Jeju [10], Majorca [11], Sardinia and Corsica [12].

Voltage Source Converters (VSC) can provide additional benefits for an islanded power system thanks to their higher controlability. Compared to LCCs, VSCs do not present commutation failure due to disturbances on the AC grid and can provide both voltage and frequency support, contributing to improve the system stability. Therefore, VSCs can operate connected to weak grids, which may represent small islands with a low number of synchronous generators. However, when the synchronous generation of the system is reduced, the inertia or short-circuit current may not be sufficient to ensure a stable operation with conventional VSC controls. As a solution, the VSC control can be improved, *e.g.* the current reference loop is modified in [13] to operate connected to grids with low short-circuit current. Also, VSCs can operate in grid-forming mode, *i.e.* generating the voltage magnitude and angle of the grid [14]. It is important to identify the operational limits of conventional VSC control techniques for frequency and voltage support and when grid-forming techniques should be applied to ensure stable operation of the islanded system. The multiterminal HVDC grid used in Zhousand islands represents an example of islanded system connected through VSC-HVDC [15].

Multi-infeed HVDC systems with LCC and VSC-HVDC links may become more common in islanded system (see Fig. 1), since VSCs can provide additional benefits for LCCs, *e.g* reduction of commutation failure or harmonic emission without large passive filters [16], and can improve the stability. Currenly, few multi-infeed systems are planned or in operation: Gotland is interconnected through a LCC and a VSC-HVDC link, whereas an additional VSC-HVDC link might be installed in Jeju [10].

This paper analyses interactions in a multi-infeed HVDC islanded system with LCC and VSC-HVDC links. In particular, frequency stability is evaluated in a case study that represents an island with two HVDC links, two synchronous generators and an aggregated load. The frequency response contribution of the HVDC links is analysed when a conventional frequency-power droop control is implemented. Also, frequency stability limits are determined when the synchronous generation of the island is reduced. Time-domain simulations in PSCAD/EMTDC have been carried out to demonstrate the frequency response of the islanded system

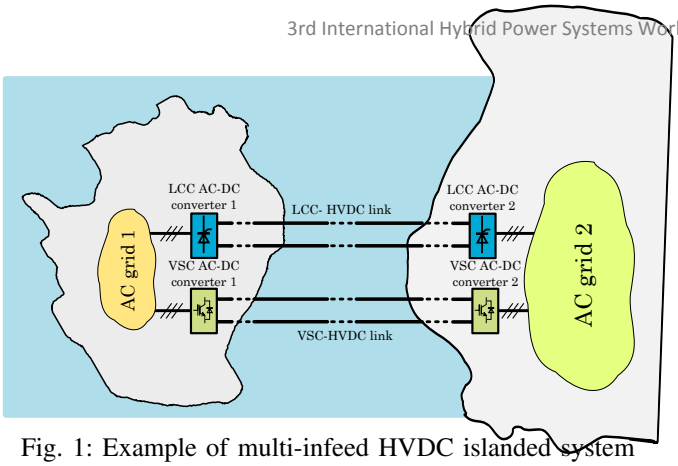

Fig. 1: Example of multi-infeed HVDC islanded system

after a sudden disconnection of synchronous generation.

II. Multi-Infeed HVDC Islanded System

Fig. 2 shows the configuration of the system under study, which represents an islanded AC grid fed by an LCC and a VSC-HVDC link importing power from a AC main grid. Switching models have been used for the inverter HVDC terminals connected to the island, while the rectifier HVDC terminals are represented as voltage sources. The islanded grid is composed by two synchronous generators that are connected to the same bus, a variable load and three overhead lines, $L1$, $L2$ and $L3$, which are represented with frequency dependent models.

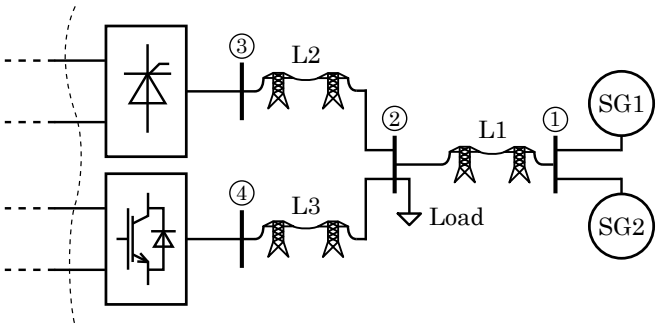

Fig. 2: Case study of multi-infeed islanded system with an LCC and a VSC-HVDC links

A. Configuration and Control of LCC-HVDC Link

The LCC-HVDC link is based on 12-pulse bridges with asymmetrical monopole configuration. The rectifier side is represented with an average model, as shown in Fig. 3, which is modelled as [17]:

$$V_{DC-r}^{LCC} = \frac{6\sqrt{2}}{\pi} T V_{AC2} \cos\alpha - I_{DC}^{LCC} \frac{6}{\pi} T\omega L_{AC} \quad (1)$$

where, V_{AC2} and ω are the line-to-line voltage and angular frequency of the AC grid, I_{DC}^{LCC} is the DC current through the LCC-HVDC link, T is the transformer ratio and L_{AC} is the equivalent inductance of the transformer. The inverter side, is represented with a detailed model including thyristors, transformers and reactive and harmonic compensation filters. A conventional operation is considered, where the LCC-rectifier controls DC current and the LCC-inverter controls DC voltage [18]. An extinction angle γ control is also implemented in the inverter side to reduce the risk of commutation failure. The control structure is based on PI controllers that define the firing angles for the thyristors, as shown in Fig. 3.

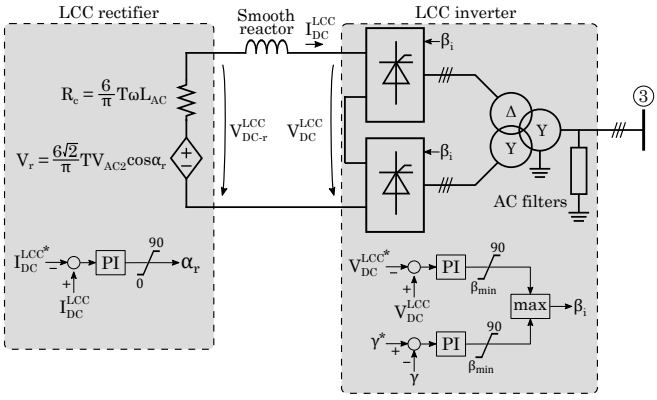

Fig. 3: Representation of LCC-HVDC link

B. Configuration and control of MMC-HVDC link

The VSC-HVDC link is based on Modular Multilevel Converters (MMC) with half-bridge submodules and asymmetrical monopole configuration. The rectifier side is modelled as a DC voltage source, as shown in Fig. 4, whereas the inverter side is represented with the MMC accelerated model presented in [19]. This MMC model represents all the submodules of the converter individually as capacitors that are connected or disconnected depending on their switching states. The VSC-HVDC link operation considers the VSC-rectifier controlling DC voltage and the VSC-inverter controlling active power and AC voltage of the islanded system. The VSC-rectifier control is not represented, whereas the VSC-inverter includes a detailed MMC control. The control strategy for the MMC is shown in Fig. 4 and is based on [20]. The main objective of the MMC control is to exchange power between the AC and DC grids, while ensuring balancing of the energy stored in all the arms without large deviations. Also, Nearest Level Modulation (NLM) is used as a modulation technique, which can reduce the average commutation frequency [21].

C. Modelling and control of synchronous generators

The synchronous generation of the islanded system is represented by two conventional steam power plants, including turbines, synchronous machines, exciters and governors, as shown in Fig. 5. The mechanical part of the generation unit is represented by single-mass models with a specific inertia.

D. Frequency control

Frequency control is based on a conventional power-frequency droop. Fig. 6 shows the control structure of the power-frequency droop implemented in the converters and synchronous generators. The power-frequency droop gain, K_{droop}, can be defined as in [17]:

$$K_{droop} = \frac{\Delta f / f_0}{\Delta P / P_0} \cdot 100 = \frac{1}{k_{fp}} \frac{P_0}{f_0} \cdot 100 \quad (2)$$

where Δf and ΔP are the frequency and power variations, f_0 is the nominal synchronous frequency, P_0 is the rated power of the converter or synchronous generator and k_{fp} is the control gain shown in Fig. 6.

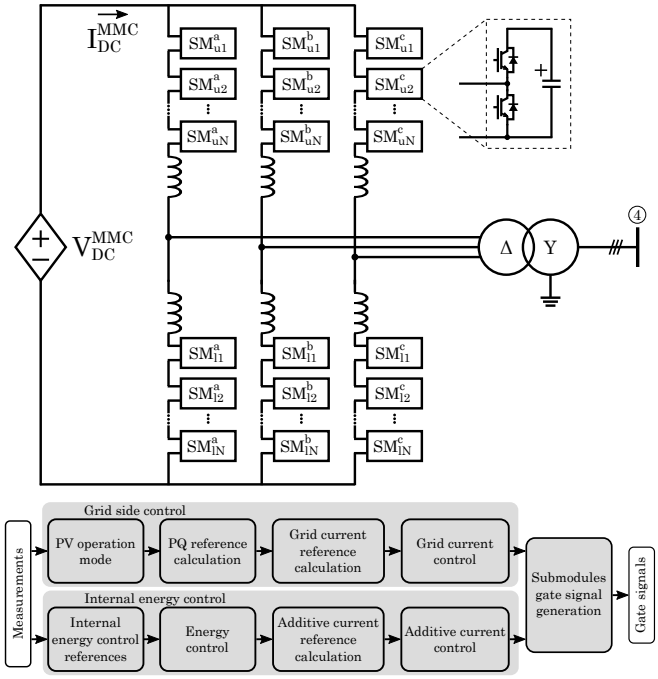

Fig. 4: MMC configuration and control

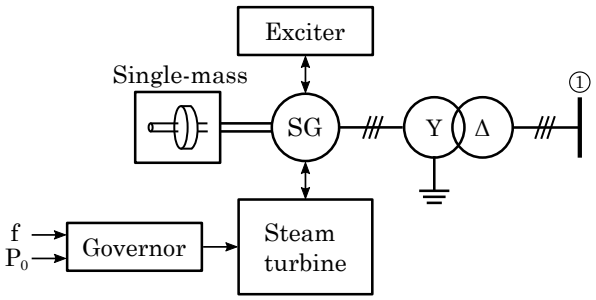

Fig. 5: Frequency response depending on the remain synchronous generation power

III. Case study

Two case studies are analysed considering the islanded systems presented in Section II and with the parameters shown Table I. First, the contribution of the HVDC links to the frequency response is analysed. Then, the frequency stability of the islanded system is evaluated by reducing the synchronous generation, *i.e.* the inertia of the system. In order to analyse the frequency response of the system, a sudden loss of synchronous generation is simulated in PSCAD/EMTDC, disconnecting generator SG2 from the system.

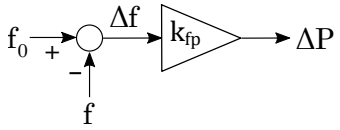

Fig. 6: Frequency response depending on the remain synchronous generation power

TABLE I: Systems parameters

Parameter	Value	Unit
AC grid voltage (RMS, ph-ph)	220	kV
LCC rated power	200	MW
MMC rated power	500	MW
Generators droop	5	%
LCC droop	2	%
MMC droop	2	%
Lines length (L1, L2 and L3)	15	km

A. Case Study 1: Contribution of HVDC links to Frequency Support

The contribution of HVDC links to frequency support of the islanded system is analysed considering the load and generation specified in Table II, where 41.7 % of the total load is supplied by synchronous generation. A sudden loss of 50 MW of synchronous generation (SG2) is considered at 1 s, which represents a 8.3% of the total generation. Different scenarios have been tested depending on the elements that contribute to frequency support:

- Only Synchronous generators (SG)
- Synchronous generators and LCC-HVDC link (SG+LCC)
- Synchronous generators and VSC-HVDC link (SG+MMC)
- Synchronous generators and both HVDC links (SG+LCC+MMC)

TABLE II: Operational parameters in first case study.

Parameter	Value	Unit
SG1 power	200	MW
SG2 power	50	MW
LCC-HVDC link power	100	MW
VSC-HVDC link power	250	MW
Load	600	MW

Fig. 7 shows the frequency response for all the scenarios. When the converters do not provide frequency support, the generator SG1 has to compensate the power imbalance caused by the loss of SG2. The frequency is reduced below 49.2 Hz, which is not within acceptable operational ranges [22]. The steady state frequency is 49.69 Hz and is reached around 20 seconds after the generation loss. It is clear that the converters can contribute significantly to the frequency support, reducing the maximum frequency deviation (the frequency is always above 49.7 Hz) and reaching the steady state in a shorter time. This is because the converters have a faster dynamic response, compared to the synchronous generators, to compensate the power imbalance after the generation loss.

B. Case Study 2: Frequency stability limits

The frequency stability limits are analysed considering a reduction in the total synchronous generation of the islanded system, *i.e.* a reduction in the total inertia. In this case study, the load is 550 MW and a sudden loss of 100 MW of synchronous generation (SG2) is applied at 1s, which represents a 18.2 % of the total generation. Initially the power transferred from the converters is the same as in the previous case study and each synchronous generator (SG1

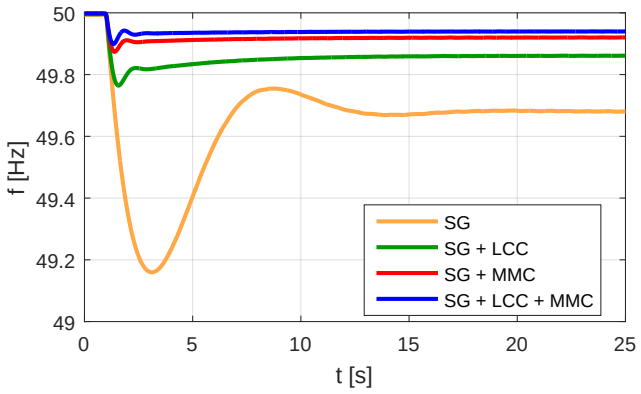

Fig. 7: Frequency response comparison with or without support of the converters

and SG2) provides 100 MW, *i.e.* 36.4 % of the total load is supplied by synchronous generation.

In order to test the frequency stability limits the generation from SG1 is reduced progressively, while the total load is maintained and replaced by additional power from the converters shared equally between the MMC and LCC. Table III shows the 4 scenarios considered in this case study, where the total synchronous generation before and after the power imbalance is indicated.

TABLE III: Scenarios to analyse frequency stability limits.

Scen.	Initial SGs (MW)	Initial SGs (%)	Final SGs (%)
1	200	36.4	18.2
2	150	27.3	9.1
3	125	22.7	4.6
4	112.5	20.5	2.3

Fig. 8 and Fig. 9 show the results of the power contribution from each synchronous generator and converter and the frequency response. When the SG2 is disconnected, SG1 starts compensating the power, reducing the frequency of the system as the mechanical torque provided by the turbine is slower than the electrical one. When this reduction on the frequency is detected by the converters, they start injecting power according to the droop control. When the synchronous generation that remains connected to the system is high enough, the converters can respond correctly to the change (see Fig. 8a). When the inertia is reduced, some oscillations appears in the power of the converters, which can be translated to frequency oscillations. When SG1 generates 50 MW, the power of the MMC begins oscillating but the system has enough damping and the effect on the frequency is not significant, as shown in Fig. 8b. When the power from SG1 is reduced to 25 MW, this oscillation is increased and the frequency is affected, as shown in Fig. 8c. The frequency of this oscillation is around 14 Hz, which is in the range of electromechanical interactions. When the power from SG is reduced to 12.5 MW, the system is is stable, but the operation is not acceptable as the large oscillations would force the disconnection of the converters, as shown in Fig. 8d. Fig. 9 shows the frequency for all the cases, where lower inertia values of the system are translated to a decrease on the minimum frequency.

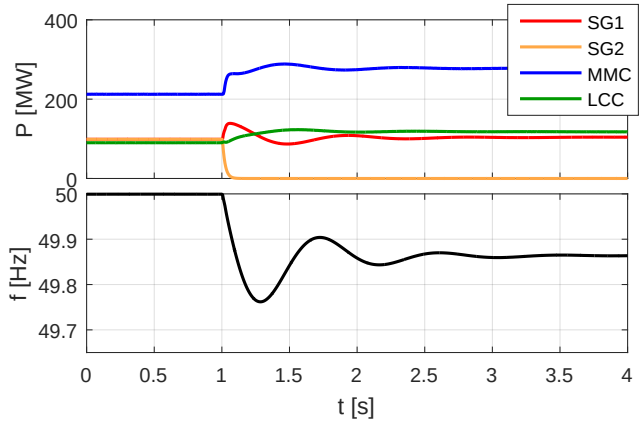

(a) Scenario 1

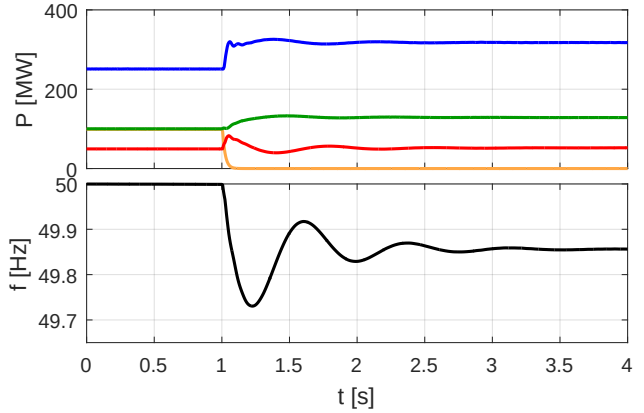

(b) Scenario 2

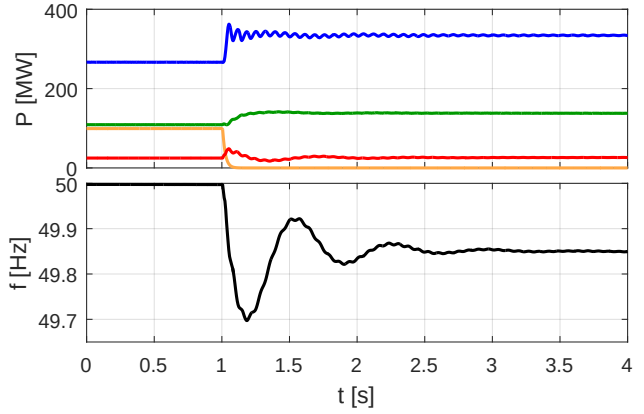

(c) Scenario 3

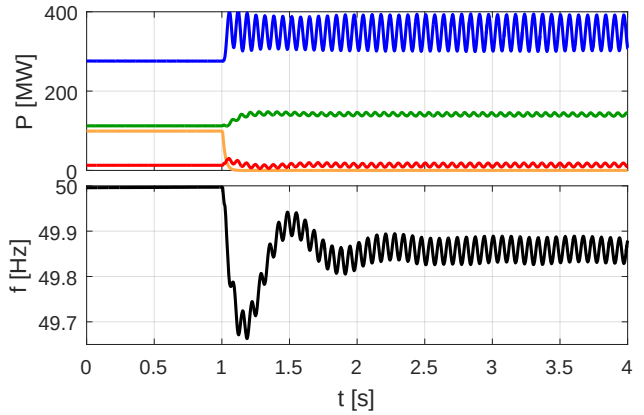

(d) Scenario 4

Fig. 8: Simulation results when the inertia of the system is reduced

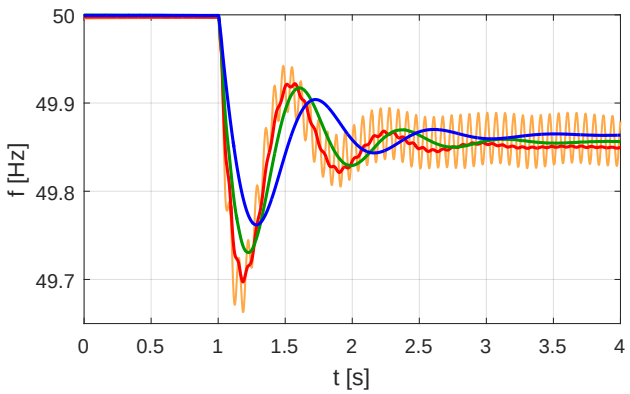

Fig. 9: Frequency response depending on the remain synchronous generation power

IV. Conclusion

This paper has presented interactions in multi-infeed HVDC islanded systems that result into frequency instability. HVDC links provide fast frequency response and reduce significantly the frequency deviations after a power imbalance caused by the loss of synchronous generation. However, when total synchronous generation is replaced by power transferred from the HVDC links the total inertia will reduced until the system becomes unstable. In a scenario with low inertia electromechanical interactions might cause frequency instability and must be studied in detail. A potential solution will be to operate the MMC as a grid-forming converter, which may avoid interactions with the synchronous generators.

Acknowledgment

This work has been funded in part by the Spanish Ministry of Economy and Competitiveness under Project ENE2015-67048-C4-1-R

References

[1] G. Li and J. Sun, "Control Hardware-in-the-Loop Simulation for Turbine Impedance Modelling and Verification," in *16th Wind Integration Workshop*, Berlin, 2017.

[2] H. Liu, X. Xie, J. He, T. Xu, Z. Yu, C. Wang, and C. Zhang, "Subsynchronous Interaction Between Direct-Drive PMSG Based Wind Farms and Weak AC Networks," *IEEE Transactions on Power Systems*, vol. 32, no. 6, pp. 4708–4720, nov 2017. [Online]. Available: http://ieeexplore.ieee.org/document/7878693/

[3] L. P. Kunjumuhammed, B. C. Pal, C. Oates, and K. J. Dyke, "Electrical oscillations in wind farm systems: Analysis and insight based on detailed modeling," *IEEE Transactions on Sustainable Energy*, vol. 7, no. 1, pp. 51–62, 2016.

[4] J.-S. Yoon, S.-Y. Kim, Y.-H. Kim, K.-C. Lee, and C.-k. Lee, "The analysis of STATCOM and SVC ccoperation effect," in *Transmission & Distribution Conference & Exposition: Asia and Pacific, 2009*, 2009.

[5] H. Saad, S. Dennetiere, and B. Clerc, "Interactions investigations between power electronics devices embedded in HVAC network," in *13th IET International Conference on AC and DC Power Transmission*, 2017.

[6] G. Andersson, P. Fischer de Toledo, and G. Liss, "HVDC Multi-Infeed Performance," pp. 1–6.

[7] CIGRE, "Systems with multiple DC infeed," *Cigré*, no. WG B4.41, pp. 14–19, 2007.

[8] C. K. Kim and G. Jang, "Operation strategy of Cheju AC network included multi-infeed HVDC system," *Journal of Electrical Engineering and Technology*, vol. 8, no. 3, pp. 393–401, 2013.

[9] G. Asplund, L. Carlsson, and O. Tollerz, "50 Years HVDC - Part II," Tech. Rep., 2003.

[10] S. Hwang, M. Yoon, and G. Jang, "Evaluation of STATCOM Capability on Transient Stability in Jeju-island with Large-scale Wind Farm," in *CIGRE: AORC Technical meeting 2014*, 2014, pp. 0–5.

[11] J. Prieto, R. Granadino, E. Betten, G. Curtotti, C. Velazquez, C. Gaebler, H. Weinkauf, S. Achenbach, and A. Galarza, "The RÓMULO project , Spanish peninsula Mallorca (243 km , 250 kV , 2x200 MW): first Spanish HVDC link," in *CIGRE: Paris 2010*, 2010.

[12] V.C. Billon ; J.P. Taisne ; V. Arcidiacono ; F. Mazzoldi, "The Corsican tapping: from design to commissioning tests of the third terminal of the Sardinia-Corsica-Italy HVDC," *IEEE Transactions on Power Delivery*, vol. 4, no. 1, pp. 794–799, 1989.

[13] A. Egea-Alvarez, S. Fekriasl, F. Hassan, and O. Gomis-Bellmunt, "Advanced Vector Control for Voltage Source Converters Connected to Weak Grids," *IEEE Transactions on Power Systems*, vol. 30, no. 6, pp. 3072–3081, 2015.

[14] J. Rocabert, A. Luna, F. Blaabjerg, and I. Paper, "Control of Power Converters in AC Microgrids," *IEEE Transactions on Power Electronics*, vol. 27, no. 11, pp. 4734–4749, 2012.

[15] C. Li, X. Hu, J. Guo, and J. Liang, "The DC grid reliability and cost evaluation with Zhoushan five-terminal HVDC case study," *Proceedings of the Universities Power Engineering Conference*, vol. 2015-Novem, 2015.

[16] N. Flourentzou, V. Agelidis, and G. Demetriades, "VSC-Based HVDC Power Transmission Systems: An Overview," *IEEE Transactions on Power Electronics*, vol. 24, no. 3, pp. 592–602, 2009. [Online]. Available: http://ieeexplore.ieee.org/lpdocs/epic03/wrapper.htm?arnumber=4773229

[17] P. Kundur, *Power System Stability and Control*, 1994.

[18] D. Jovcic and K. Ahmed, *High Voltage Direct Current Transmission: Converters, Systems and DC Grids*. Wiley, 2015.

[19] J. Xu, C. Zhao, W. Liu, and C. Guo, "Accelerated Model of Modular Multilevel Converters in PSCAD/EMTDC," *IEEE Transactions on Power Delivery*, vol. 28 (1), pp. 129–136, jan 2013.

[20] E. Prieto-Araujo, A. Junyent-Ferré, C. Collados-Rodríguez, G. Clariana-Colet, and O. Gomis-Bellmunt, "Control design of Modular Multilevel Converters in normal and AC fault conditions for HVDC grids," *Electric Power Systems Research*, vol. 152, pp. 424–437, 2017. [Online]. Available: http://dx.doi.org/10.1016/j.epsr.2017.06.020

[21] Q. Tu and Z. Xu, "Impact of sampling frequency on harmonic distortion for modular multilevel converter," *IEEE Transactions on Power Delivery*, vol. 26, no. 1, pp. 298–306, 2011.

[22] ENTSO-E, "Network Code on Load-Frequency Control and Reserves," 2013. [Online]. Available: http://networkcodes.entsoe.eu/wp-content/uploads/2013/08/130628-NC_LFCR-Issue1.pdf